THE JOURNAL OF BIOLOGICAL CHEMISTRY
Vol. 278, No. 16, Issue of April 18, pp. 13898–13904, 2003
Printed in U.S.A.

Nerve Growth Factor Protects against 6-Hydroxydopamine-induced Oxidative Stress by Increasing Expression of Heme Oxygenase-1 in a Phosphatidylinositol 3-Kinase-dependent Manner*

Received for publication, September 6, 2002, and in revised form, February 7, 2003
Published, JBC Papers in Press, February 10, 2003, DOI 10.1074/jbc.M209164200

Marta Salinas‡§, Raquel Diaz¶‖, Nader G. Abraham, Carlos M. Ruiz de Galarreta¶, and Antonio Cuadrado‡ ‡‡**

*From the ‡Instituto de Investigaciones Biomédicas and the Departamento de Bioquímica, Facultad de Medicina, Universidad Autónoma de Madrid, 28029 Madrid, Spain, the ¶Departamento de Bioquímica, Facultad de Medicina, Universidad de las Palmas de Gran Canaria, 35016 Gran Canaria, Spain, and the **Department of Pharmacology, New York Medical College, Valhalla, New York 10595*

The survival signal elicited by the phosphatidylinositol 3-kinase (PI3K)/Akt1 pathway has been correlated with inactivation of pro-apoptotic proteins and attenuation of the general stress-induced increase in reactive oxygen species (ROS). However, the mechanisms by which this pathway regulates intracellular ROS levels remain largely unexplored. In this study, we demonstrate that nerve growth factor (NGF) prevents the accumulation of ROS in dopaminergic PC12 cells challenged with the Parkinson's disease-related neurotoxin 6-hydroxydopamine (6-OHDA) by a mechanism that involves PI3K/Akt-dependent induction of the stress response protein heme oxygenase-1 (HO-1). The effect of NGF was mimicked by induction of HO-1 expression with $CoCl_2$; by treatment with bilirubin, an end product of heme catabolism; and by infection with a retroviral expression vector for human HO-1. The relevance of HO-1 in NGF-induced ROS reduction was further demonstrated by the evidence that cells treated with the HO-1 inhibitor tin-protoporphyrin or infected with a retroviral expression vector for antisense HO-1 exhibited enhanced ROS release in response to 6-OHDA, despite the presence of the neurotrophin. Inhibition of PI3K prevented NGF induction of HO-1 mRNA and protein and partially reversed its protective effect against 6-OHDA-induced ROS release. By contrast, cells transfected with a membrane-targeted active version of Akt1 exhibited increased HO-1 expression, even in the absence of NGF, and displayed a greatly attenuated production of ROS and apoptosis in response to 6-OHDA. These observations indicate that the PI3K/Akt pathway controls the intracellular levels of ROS by regulating the expression of the antioxidant enzyme HO-1.

High levels of reactive oxygen species (ROS)[1] induce cell death in the nervous system and have been associated with a number of pathologies such as Parkinson's disease (1). Neurotrophins, including nerve growth factor (NGF), promote survival of target neurons and attenuate ROS-induced cell death (2). A prominent mechanism involved in NGF-induced cell survival consists of the activation of phosphatidylinositol 3-kinase (PI3K) and its downstream effectors, including the protein kinase B/Akt family of Ser/Thr kinases (3–5). This pathway exerts protective actions against oxidative damage in central and peripheral neurons (6). In this context, neuregulin prevents H_2O_2 induction of ROS in a PI3K-dependent manner (7). Loss of oxidative stress tolerance with aging has been linked in part to reduced Akt kinase activity in old rats (8). Concerning neurodegeneration, we have recently reported the protective effect of active Akt1 against peptides of β-amyloid protein, characteristic of senile plaques found in the brains of Alzheimer's patients (9); against the Parkinson's disease-inducing toxin 1-methyl-4-phenylpyridinium (10); and against apoptotic concentrations of H_2O_2 (11). In these cases, expression of a constitutively active version of Akt prevented the increase in ROS that follows treatment of PC12 cells with these toxins.

However, although those studies support an involvement of Akt in counteracting oxidative damage in neurons, a direct role of this pathway in the regulation of canonical antioxidant defenses, represented by the superoxide dismutases and/or the catalase/glutathione peroxidase system, has not been identified. On the contrary, recent reports on the dauer stage of *Caenorhabditis elegans* and quiescent mammalian cells indicate that, in the absence of active PI3K and Akt, forkhead transcription factors (DAF-16 and FOXO3a, respectively) increase the expression of mitochondrial superoxide dismutase (12, 13). Moreover, mutations in the *daf-2* network of *C. elegans* that inactivate PI3K and Akt lead to up-regulation of a cytosolic catalase (14); and in *Drosophila melanogaster*, inactivation of this pathway results in increased superoxide dismutase activity (15). Therefore, activation of PI3K and Akt must lead to up-regulation of other ROS detoxification systems.

In addition to the well characterized ROS scavenger systems mentioned above, emerging evidence supports a role for heme oxygenase (HO) enzymes as important components of the cellular antioxidant armamentarium (16, 17). The heme oxygenase family is composed of at least two well characterized isoenzymes: inducible HO-1 and constitutive HO-2. HO-1, also known as HSP32 (heat shock protein of 32 kDa), is a stress

* This work was supported in part by Grant SAF2001-0546 from the Spanish Ministry of Education and Grant 08.5/0048/2001 from the Comunidad Autónoma de Madrid. The costs of publication of this article were defrayed in part by the payment of page charges. This article must therefore be hereby marked "*advertisement*" in accordance with 18 U.S.C. Section 1734 solely to indicate this fact.

§ Recipient of a fellowship (Formación de Personal Investigador) from the Spanish Ministry of Education.

‖ Supported by Grant FEDER IF97/0602.

‡‡ To whom correspondence should be addressed: Dept. de Bioquímica, Facultad de Medicina, Universidad Autónoma de Madrid, Arzobispo Morcillo 4, 28029 Madrid, Spain. Tel.: 34-91-397-5327; Fax: 34-91-585-4401; E-mail: antonio.cuadrado@uam.es.

[1] The abbreviations used are: ROS, reactive oxygen species; NGF, nerve growth factor; PI3K, phosphatidylinositol 3-kinase; HO, heme oxygenase; 6-OHDA, 6-hydroxydopamine; EGFP, enhanced green fluorescent protein; myr, myristoylated; HE, hydroethidine; PE, phycoerythrin; 7-AAD, 7-aminoactinomycin D.

response protein whose expression is induced in practically all tissues and cells tested in response to multiple oxidative insults such as heme, UV light, heavy metals, glutathione depletion, and H_2O_2. This enzyme catalyzes the stepwise degradation of heme to release free iron and equimolar concentrations of carbon monoxide (CO) and the linear tetrapyrrol biliverdin, which is converted to bilirubin by the enzyme biliverdin reductase. Many reports have established the potent antioxidant activity of biliverdin and bilirubin and the cytoprotective actions of CO on vascular endothelium and nerve cells (16–19). Therefore, it is now widely accepted that induction of heme catabolism represents an adaptive, and ultimately protective, response to oxidative injury. Of particular relevance to this study, it has also been shown that the normally low levels of HO-1 expression in neurons (20, 21) dramatically increase after formation of brain neurofibrillary tangles in Alzheimer's patients (22) and neuronal Lewy bodies in the substantia nigra of Parkinson's patients (23) and that cerebellar granular neurons overexpressing HO-1 are resistant to glutamate-mediated oxidative stress (24).

The progressive deterioration of catecholaminergic cells in Parkinson's patients has been attributed, at least in part, to the high vulnerability of these cells to oxidative damage. One potential source of ROS in the substantia nigra includes the autoxidation of the neurotransmitter dopamine to generate 6-hydroxydopamine (6-OHDA) (25). In fact, 6-OHDA is present in rodent and human brains and has been widely used in experimental models of Parkinson's disease. Evidences derived from *in vivo* and *in vitro* experimental models of this disease have demonstrated that 6-OHDA neurotoxicity involves oxidative damage to catecholaminergic neurons (26) via the generation of hydroxyl radicals, monoamine oxidase-mediated formation of H_2O_2, and mitochondrial generation of superoxide (25).

With the aim to determine whether PI3K and Akt modulate the heme oxygenase system of ROS detoxification, we analyzed the effect of NGF on the regulation of HO-1 expression in catecholaminergic PC12 cells. We show that NGF-induced activation of PI3K/Akt up-regulates the expression and activity of HO-1, which, in turn, provides protection against 6-OHDA-induced oxidative damage in PC12 cells. These data contribute to revealing the mechanism whereby NGF and PI3K/Akt provide protection against oxidative injury and may be potentially relevant in the development of new therapies for neurodegenerative disorders such as Parkinson's disease.

EXPERIMENTAL PROCEDURES

Cell Culture, Transfections, and Reagents—PC12 cells (a gift of Dr. H. Kleinman, NIDCR, National Institutes of Health, Bethesda, MD) were grown in Dulbecco's modified Eagle's medium supplemented with 7.5% fetal bovine serum, 7.5% heat-inactivated horse serum, and 80 μg/ml gentamycin. Eukaryotic expression vectors for enhanced green fluorescent protein (EGFP) and myristoylated (myr)-EGFP-Akt1 have been described elsewhere (13). Stable transfection of PC12 cells was performed with Superfect transfection reagent (QIAGEN Inc., Valencia, CA) according to the manufacturer's instructions. The amphotropic retroviral packaging cell lines PT67 and PA317 (Clontech) were used to collect replication-deficient retroviruses containing the retroviral vector (LXSN) expressing human HO-1 antisense cDNA under the control of the human HO-1 promoter (LSN-HOP-HHO-1-AS) and human HO-1 in the sense orientation (LSN-HHO-1), respectively. These retroviral constructs have been described elsewhere (27). PC12 cells infected with the pLNCX retroviral vector (a generous gift of Dr. R. Perona, Instituto de Investigaciones Biomédicas, Universidad Autónoma de Madrid) were used as controls for HO-1 infections. Transfected and infected cells were selected in 0.5 mg/ml G418. The reagents employed were NGF (Peprotec, Rocky Hill, NJ), tin-protoporphyrin (Protoporphyrin Products, Logan, UT), and 6-OHDA, actinomycin D, cycloheximide, LY294002, hemin, bilirubin, and $CoCl_2$ (Sigma).

HO Assays—Microsomal HO-1 activity was determined spectrophotometrically in PC12 cell microsomes incubated for 1 h in the dark at 37 °C in the presence of hemin (10 μM), NADPH (20 μM), and 1 mg of protein from rat liver cytosol as a source of biliverdin reductase (28). Reactions were terminated by adding 1 ml of chloroform, and the concentration of bilirubin was determined from the difference in absorbance between 464 and 530 nm using an extinction coefficient of 40 $mM^{-1}\ cm^{-1}$.

Analysis of mRNA Levels by Reverse Transcriptase-PCR—Total cellular RNA was extracted using TRIzol reagent (Invitrogen) (29). Equal amounts (1 μg) of RNA from the different treatments were reverse-transcribed (75 min, 42 °C) using Superscript II reverse transcriptase (Invitrogen). Amplification of cDNA was performed in 25 μl of PCR buffer (10 mM Tris-HCl, 50 mM KCl, 5 mM $MgCl_2$, and 0.1% Triton X-100, pH 9.0) containing 2.5 mM digoxigenin-dUTP, 0.6 units of *Taq* DNA polymerase, and 30 pmol of synthetic gene-specific primers for HO-1 (forward, 5′-AAGGCTTTAAGCTGGTGATGG-3′; and reverse, 5′-AGCGGTGTCTGGGATGAACTA-3′). To ensure that equal amounts of reverse-transcribed RNA were added to the PCR, the glyceraldehyde-3-phosphate dehydrogenase or β-actin housekeeping gene was amplified using commercially available oligonucleotides (Clontech). After an initial denaturation step (4 min, 94 °C), amplification of each cDNA was performed for 17, 19, 21, 23, and 25 cycles (HO-1, glyceraldehyde-3-phosphate dehydrogenase, or β-actin) using a thermal profile of 1 min at 94 °C (denaturation), 1 min at 58 °C (annealing), and 1 min at 72 °C (elongation). The optimal number of cycles within the linear range of amplification were selected as 23 for HO-1 and 19 for glyceraldehyde-3-phosphate dehydrogenase or β-actin (data not shown). The amplified PCR products were resolved by 1.8% agarose gel electrophoresis and transferred to nylon membranes. Chemiluminescence detection was performed with a digoxigenin luminescence detection kit (Roche Molecular Biochemicals, Basel, Switzerland).

Immunoblotting—Primary anti-HO-1 antibodies were purchased from Stressgen and Oxys. Anti-protein-disulfide isomerase antibodies were a gift from Dr. J. G. Castaño (Instituto de Investigaciones Biomédicas, Universidad Autónoma de Madrid-Consejo Superior de Investigaciones Científicas). Cells were grown in 60-cm plates, washed once with cold phosphate-buffered saline, and lysed on ice with 200 μl of lysis buffer (1% Nonidet P-40, 10% glycerol, 137 mM NaCl, 20 mM Tris-HCl, pH 7.5, 1 μg/ml leupeptin, 1 mM phenylmethylsulfonyl fluoride, 20 mM NaF, 1 mM sodium pyrophosphate, and 1 mM Na_3VO_4). Lysates were precleared by centrifugation, resolved by SDS-PAGE, and transferred to Immobilon-P membranes (Millipore Corp., Madrid, Spain). Blots were analyzed with anti-HO-1 antibodies (1:1000). Appropriate peroxidase-conjugated secondary antibodies (1:10,000) were used to detect the proteins of interest by enhanced chemiluminescence. Relative protein levels were determined by scanning densitometry and analysis with NIH Image software.

Confocal Microscopy—Cells were seeded on glass-bottom 35-mm plates (Willco, Amsterdam, The Netherlands). Following overnight serum starvation, cells were incubated with 40 μM 6-OHDA for 6 h or with 1 mM H_2O_2 for 45 min and afterward with 2 μM hydroethidine (HE) (Molecular Probes, Inc., Eugene, OR) for 1 h at 37 °C. Confocal microscopy was performed using a Leica SP2 system. For HE, we used an excitation wavelength of 488 nm, and fluorescence was detected at wavelengths between 557 and 740 nm. For Hoechst 33258, we used an excitation wavelength of 351 nm, and fluorescence was detected at wavelengths between 386 and 512 nm.

Flow Cytometry—A FACScan flow cytometer (BD Biosciences, Madrid) was used to analyze fluorescence from HE (band pass 575/24 nm), annexin V-phycoerythrin (PE) (band pass 620/22 nm), and 7-aminoactinomycin D (7-AAD) (band pass 575/24 nm). Intracellular ROS were detected with HE. Cells were detached from the plates, washed with phosphate-buffered saline, incubated with 2 μM HE for 1 h at 37 °C, and analyzed immediately. Base-line incorporation of the probe was determined in serum-starved cells incubated in 2 μM HE at 4 °C. Variations in HE fluorescence between experiments were attributed to slight differences in the photomultiplier parameters used during data acquisition and to small differences among batches of HE. For apoptosis assays, floating and attached cells were transferred to conical tubes and spun at 300 × *g* for 10 min. Cells were resuspended in annexin V binding buffer (10 mM HEPES-NaOH, pH 7.4, 140 mM NaCl, and 2.5 mM $CaCl_2$) at 10^6 cells/ml. Cells were incubated for 15 min at 25 °C in a 1:20 solution of annexin V-PE (Pharmingen, Madrid) supplemented with 1 μg/ml 7-AAD (Sigma) and analyzed immediately.

Statistics—Student's *t* test was used to assess differences between groups. A p value of <0.05 was considered significant. Unless indicated, all experiments were performed al least three times with similar results. The values in graphs correspond to the average of at least three samples. Bars indicate S.D.

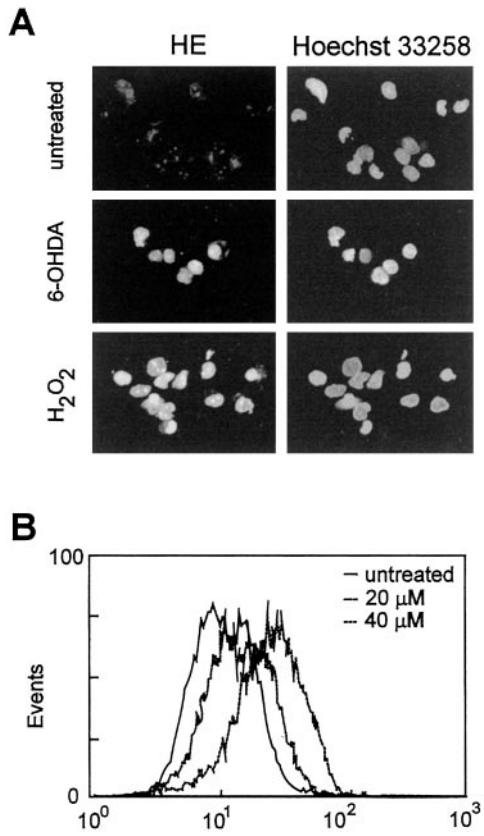

FIG. 1. **6-OHDA induces a rise in ROS in PC12 cells as determined by HE staining.** *A*, confocal microscopy pictures of representative fields from untreated and 6-OHDA- and H_2O_2-treated cells stained with HE and Hoechst 33258. Serum-starved PC12 cells were treated with 40 μM 6-OHDA for 6 h or with 1 mM H_2O_2 for 45 min, and 2 μM HE was added during the last hour of the experiment. *B*, quantitative determination by flow cytometry of 6-OHDA-induced oxidative stress by HE staining. Cells were treated as described for *A* with the indicated concentrations of 6-OHDA. A representative sample of 10,000 cells is shown for untreated and 20 and 40 μM 6-OHDA-treated cells.

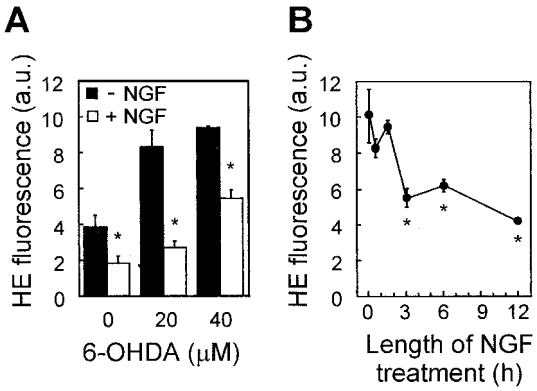

FIG. 2. **NGF antagonizes the oxidant effect of 6-OHDA.** *A*, NGF prevents 6-OHDA induction of ROS. Serum-starved cells were treated with 20 ng/ml NGF for 16 h, and 6-OHDA and HE were added for the last 6 and 1 h, respectively. *B*, prevention of 6-OHDA-induced ROS by NGF depends on the length of the NGF pretreatment. Serum-starved cells were incubated with 20 ng/ml NGF for the indicated times. They were then treated with 40 μM 6-OHDA for 6 h and with HE for 1 h. *Asterisks* denote $p < 0.001$, NGF-treated versus untreated groups. *a.u.*, absorbance units.

RESULTS

6-OHDA Induces ROS Generation in PC12 Cells—To assess variations in ROS production, we used the ROS-sensitive fluorescent probe HE, a well established sensor of oxidative stress, most specific of superoxide anion (10, 30, 31). Mitochondria are the primary sites of HE oxidation; and once converted to ethidine, this product accumulates intercalated into nucleic acids at the nucleus (31). Serum-starved PC12 cells were treated with 40 μM 6-OHDA for 6 h or with 1 mM H_2O_2 for 45 min as a control of oxidative stress, and 2 μM HE was added for 1 h. As shown in Fig. 1*A*, counterstaining of these cells with the nuclear dye Hoechst 33258 and analysis with confocal microscopy evidenced HE accumulation mostly in the nuclei of cells submitted to oxidative damage. We then quantified the incorporation of HE in 6-OHDA-treated cells by flow cytometry as shown in Fig. 1*B*. Untreated cells exhibited weak HE incorporation, indicating that the basal amount of ROS in these cells is low. By contrast, 6-OHDA induced a dose-dependent incorporation of the probe. Similar results were obtained with the green-emitting fluorophore 2′,7′-dichlorodihydrofluorescein diacetate (data not shown). However, because heme and hemoproteins may interfere with the oxidation of this dye in a ROS-independent manner (32), we concentrated the rest our work on HE.

Next, we analyzed the effect of NGF on prevention of 6-OHDA-induced release of ROS. As shown in Fig. 2*A*, a 16-h pretreatment with 20 ng/ml NGF significantly reduced the 6-OHDA-induced incorporation of HE, indicating that NGF attenuates ROS production. Moreover, as shown in Fig. 2*B*, this effect was dependent on the length of NGF pretreatment. Thus, attenuation of ROS release by NGF required the presence of this neurotrophin at least 3 h prior to the addition of 6-OHDA. These results suggest that NGF induces the expression of a gene(s) essential to ROS antagonism.

NGF Up-regulates HO-1 Expression—Considering that HO-1 is an inducible enzyme with strong antioxidant properties, we studied the effect of NGF on the expression of this protein. Treatment of PC12 cells for 6 h with NGF resulted in a 2–3-fold increase in HO activity (Fig. 3*A*). This increase was sensitive to pretreatment with actinomycin D or cycloheximide, suggesting that NGF enhances the expression of the inducible heme oxygenase isoform, HO-1. Indeed, as shown in Fig. 3 (*B* and *C*), the increase in HO activity correlated with increased levels of HO-1 mRNA and protein. Moreover, the increase in mRNA was also sensitive to cycloheximide, suggesting, in agreement with other studies (33, 34), that induction of HO-1 transcription involves *de novo* protein synthesis. Moreover, as shown in Fig. 3*D*, NGF markedly elevated HO-1 mRNA, reaching a maximum within 3 h of treatment and declining by 9 h of NGF exposure. In addition, induction of HO-1 protein by NGF was delayed (Fig. 3*E*). There was a slight increase observed at 1.5–3 h, with a maximum 6–8-fold elevation at 9 h; but HO-1 protein levels remained elevated for at least for 12 h after NGF stimulation. NGF failed to stimulate HO-2 expression (data not shown), further indicating that this neurotrophic factor specifically up-regulates the HO-1 isoform.

Induction of HO-1 Expression and Exogenous Addition of Bilirubin Attenuate ROS Generation by 6-OHDA—To assess the relevance of HO-1 in 6-OHDA detoxification, we treated PC12 cells with $CoCl_2$, a well established inducer of HO-1 expression that promotes depletion of the intracellular GSH pool and does not appear to significantly alter the activity of other antioxidant enzymes, including superoxide dismutase, catalase, and glutathione peroxidase (35). Heme oxygenase expression was induced in PC12 cells following incubation with $CoCl_2$ for 12 h as indicated in Fig. 4*A*. Plateau induction of HO-1 protein was observed with ~100 μM $CoCl_2$. Contrary to hemin, another commonly used inducer of HO-1, $CoCl_2$ did not display significant toxicity, at least for the length of these experiments (data not shown). Following 12 h of $CoCl_2$ induction of HO-1, cells were treated with 6-OHDA as indicated in

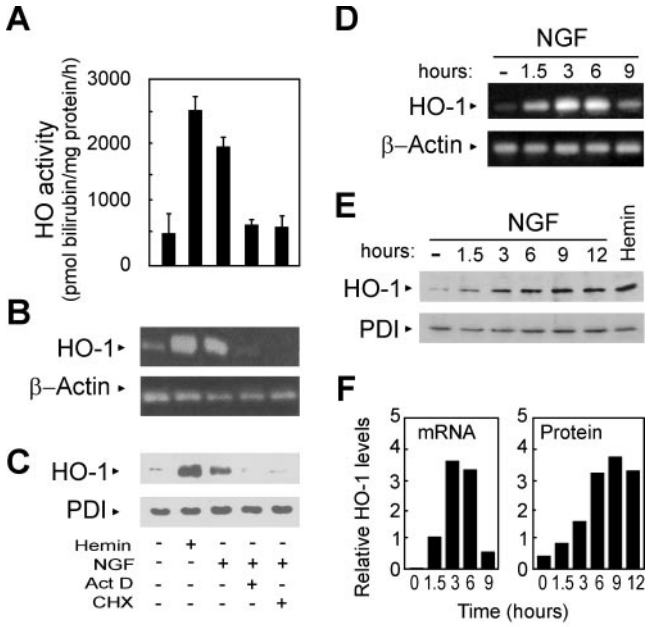

FIG. 3. **NGF induces HO-1 expression.** *A*, heme oxygenase activity of PC12 cells treated with hemin, NGF, actinomycin D (*Act D*), and cycloheximide (*CHX*) as indicated. *B*, semiquantitative reverse transcriptase-PCR showing induction of HO-1 mRNA. *Upper panel*, HO-1 mRNA; *lower panel*, β-actin mRNA used for normalization. *C*, immunoblot showing induction of HO-1 protein. *Upper panel*, blot with anti-HO-1 antibodies; *lower panel*, blot with anti-protein-disulfide isomerase (*PDI*) antibodies showing a similar amount of protein/lane. For *A–C*, serum-starved cells were untreated or pretreated with 50 μM cycloheximide or 10 μg/ml actinomycin D for 2 h prior to the addition of 50 μM hemin or 20 ng/ml NGF for an additional 6 h. *D*, time course of HO-1 mRNA expression by NGF. *Upper panel*, semiquantitative reverse transcriptase-PCR showing HO-1 mRNA; *lower panel*, β-actin mRNA used for normalization. *E*, time course of HO-1 protein expression by NGF. *Upper panel*, immunoblot with anti-HO-1 antibodies; *lower panel*, immunoblot with anti-protein-disulfide isomerase antibodies showing a similar amount of protein/lane. *F*, densitometric quantification of relative HO-1 mRNA and protein levels after treatment with NGF. For *D* and *E*, serum-starved cells were treated with 20 ng/ml NGF and then analyzed for HO-1 mRNA expression and protein at the indicated times.

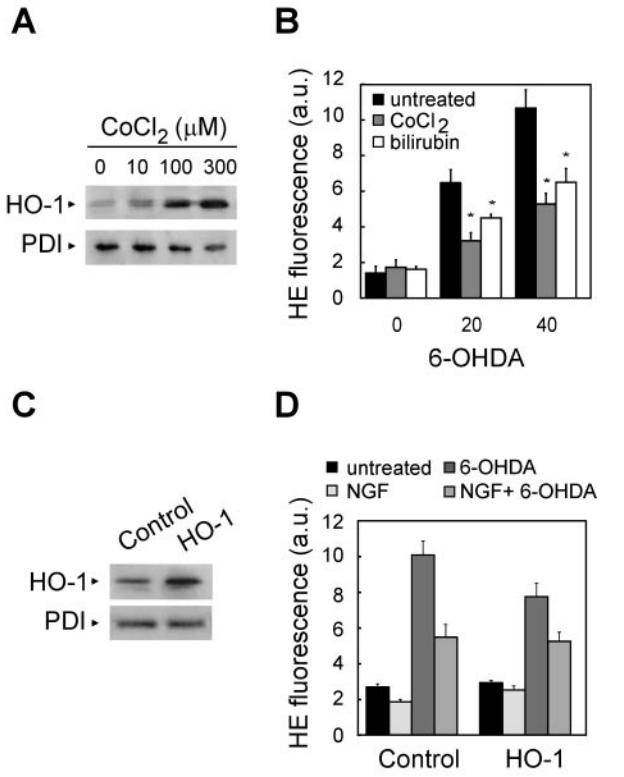

FIG. 4. **Pharmacological induction of HO-1 expression with $CoCl_2$ and moderate overexpression of HO-1 with a retroviral expression vector attenuate 6-OHDA-induced oxidative stress.** *A*, dose effect of $CoCl_2$ on HO-1 expression. *Upper panel*, immunoblot with anti-HO-1 antibodies; *lower panel*, immunoblot with anti-protein-disulfide isomerase (*PDI*) antibodies showing a similar amount of protein/lane. *B*, HE staining of 6-OHDA-treated cells in the presence of $CoCl_2$ or bilirubin. Serum-starved cells were pretreated with 100 μM $CoCl_2$ or 10 μM bilirubin for 12 h and then treated with 40 μM 6-OHDA for 6 h and 2 μM HE for 1 h. Cells were analyzed for HE staining by flow cytometry. *Asterisks* denote $p < 0.001$, control versus $CoCl_2$- or bilirubin-treated groups. *C*, immunoblot showing HO-1 levels in control and LSN-HHO-1-infected cells. Densitometric analysis of three immunoblots indicated a 2.3 ± 0.3-fold increase in HO-1 protein over the level in control non-infected cells. *D*, HE staining of control and HO-1-overexpressing cells treated with NGF and 6-OHDA. Serum-starved cells were untreated or treated with 20 ng/ml NGF for 16 h and then treated with 40 μM 6-OHDA for 6 h. Cells were incubated with HE for 1 h and analyzed by flow cytometry. *a.u.*, absorbance units.

Fig. 4*B*. $CoCl_2$ pretreatment strongly attenuated the production of ROS in the presence of 6-OHDA. To further confirm that the $CoCl_2$ protection was due to induction of HO-1, we analyzed the protective effect of bilirubin. Serum-starved cells were pretreated with 10 μM bilirubin for 12 h prior to the treatment with 6-OHDA. As shown in Fig. 4*B*, bilirubin also significantly attenuated the 6-OHDA induction of ROS, although to a lesser extent compared with $CoCl_2$. These results indicate that induction of HO-1 prevents ROS production by 6-OHDA.

Moderate Overexpression of HO-1 Attenuates 6-OHDA-induced ROS Production—We also overexpressed HO-1 in PC12 cells and determined its effect on 6-OHDA-induced HE fluorescence. PC12 cells were infected with the retroviral expression vector LSN-HHO-1, which has been described previously (27). We could not find cell clones with levels of HO-1 overexpression higher than 2–3-fold, suggesting that higher constitutive levels of HO activity may be deleterious (see "Discussion"), probably as a result of the depletion of intracellular heme reservoirs. A pool of five clones overexpressing HO-1 by 2.3 ± 0.3-fold (Fig. 4*C*) was used to assess the relevance of this enzyme in the 6-OHDA-induced production of ROS. Although modest, comparative levels of overexpression conferred protection against glutamate-mediated oxidative stress in neurons of transgenic mice (24). As shown in Fig. 4*D*, HO-1-overexpressing cells exhibited a 6-OHDA-induced HE incorporation that was intermediate between that induced by the toxin in control untreated and NGF-treated cells. These results further suggest an antioxidant effect of HO-1. Interestingly, NGF produced a similar attenuation of ROS in both control and HO-1-overexpressing cells in the presence of 6-OHDA, suggesting that the levels of HO-1 induced by the neurotrophin may be already at saturating doses. An additional interpretation might be that NGF induces other antioxidant genes or pathways that, in concert with HO-1, facilitate maximum protection against 6-OHDA-induced ROS (see "Discussion").

NGF Does Not Prevent 6-OHDA-generated ROS in HO-1-depleted Cells—To determine the relevance of HO-1 induction in the NGF protection against oxidative stress, we analyzed the effect of pharmacological inhibition of heme oxygenase with tin-protoporphyrin, a competitive inhibitor of HO-1. PC12 cells were treated with 20 ng/ml NGF and various tin-protoporphyrin concentrations in combination as indicated in Fig. 5*A*. Tin-protoporphyrin alone dose-dependently increased HE incorporation, indicating that inhibition of heme oxygenase increases cellular ROS levels. Interestingly, NGF could not prevent ROS generation in the presence of tin-protoporphyrin either in untreated cells or in cells treated with 6-OHDA, particularly at the highest doses.

We also analyzed the 6-OHDA-induced HE incorporation in

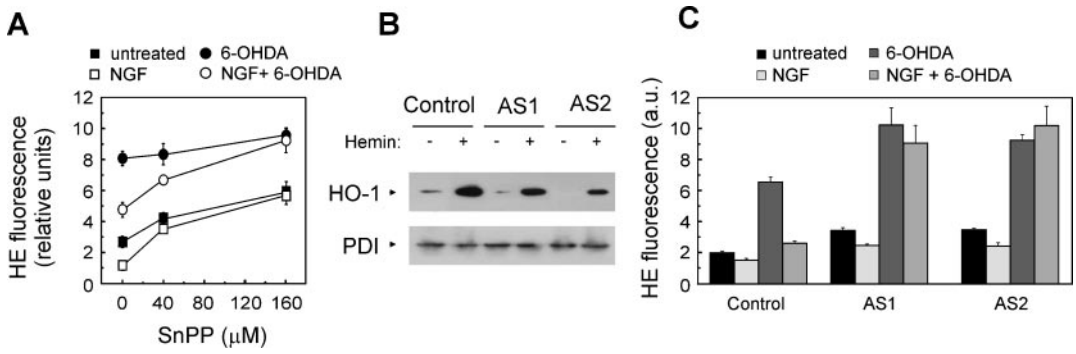

FIG. 5. **Pharmacological inhibition of heme oxygenase with tin-protoporphyrin and depletion of HO-1 with an antisense HO-1 retroviral construct abolish the protective effect of NGF against 6-OHDA-induced production of ROS.** *A*, obstruction of the antioxidant effect of NGF through inhibition of HO-1. Serum-starved cells were co-treated with 20 ng/ml NGF and the indicated concentrations of the HO-1 inhibitor tin-protoporphyrin (*SnPP*) for 16 h. They were then treated with 40 μM 6-OHDA for 6 h as indicated. Finally, cells were treated with 2 μM HE for 1 h and analyzed by flow cytometry. *B*, basal and hemin-induced levels of HO-1 protein in control PC12 cells and in two clones (AS1 and AS2) stably transduced with antisense retroviral vector LSN-HOP-HHO-1-AS. *Upper panel*, immunoblot with anti-HO-1 antibodies; *lower panel*, immunoblot with anti-protein-disulfide isomerase (*PDI*) antibodies showing a similar amount of protein/lane. Serum-starved cells were untreated or treated with 50 μM hemin for 6 h. Densitometric analysis of three immunoblots indicated reductions in the levels of total HO-1 to 54 ± 8% (AS1) and to 46 ± 12% (AS2) compared with control cells. *C*, comparison of HE staining in control, AS1, and AS2 cells treated with 6-OHDA in the presence or absence of NGF. Serum-starved cells were untreated or pretreated with 20 ng/ml for 12 h and then treated with 6-OHDA for 6 h. Cells were incubated with HE for 1 h and analyzed by flow cytometry. *a.u.*, absorbance units.

cells retrovirally transduced with antisense HO-1 constructs. The antisense retroviral expression vector for HO-1 under the control of its own promoter (LSN-HOP-HHO-1-AS) has been described previously (27). In agreement with previous reports (36), cells transfected with this antisense constructs grew more slowly (data not shown), suggesting abnormalities in cell cycle progression. Fig. 5*B* shows the endogenous levels of HO-1 in control PC12 cells and in two clones (AS1 and AS2) selected after retroviral transduction with LSN-HOP-HHO-1-AS. Both cell clones exhibited lower HO-1 protein levels compared with control cells (54 ± 8 and 46 ± 12% of the control for AS1 and AS2, respectively). Moreover, hemin yielded lower HO-1 protein levels in both antisense clones, indicating that HO-1 expression is impaired in these cells. We then analyzed the levels of 6-OHDA-induced incorporation of HE as shown in Fig. 5*C*. Treatment with 40 μM 6-OHDA induced a significantly higher incorporation of HE in the antisense clones compared with control cells, indicative of stronger production of ROS in the HO-1-depleted cells. Interestingly, pretreatment with NGF for 16 h did not prevent 6-OHDA induction of ROS in either of the antisense HO-1-transduced cells. These observations suggest that induction of HO-1 is essential for NGF to attenuate 6-OHDA-induced production of ROS; and because both antisense clones still harbor a fraction of HO-1 protein, it is likely that cells require a threshold amount of HO-1, above that present in these cells, to be efficiently protected against this neurotoxin. Taken together, these results further support a role for HO-1 in the NGF-induced antioxidant response.

NGF Induces HO-1 Expression in a PI3K- and Akt-dependent Manner—Next, we investigated the contribution of the NGF-activated PI3K/Akt survival pathway to the induction of HO-1 expression. For this purpose, PC12 cells were transfected with either a control expression vector for EGFP or a membrane-targeted active fusion of EGFP and Akt1 (myr-EGFP-Akt1), which has been described previously (13). The main advantage of using these constructs is to select transfected PC12 cells by preparative cell sorting. Serum-starved control EGFP cells were pretreated for 15 min with 40 μM LY294002, an inhibitor of PI3K, and then stimulated with 20 ng/ml NGF for 6 h. As shown in Fig. 6, the PI3K inhibitor significantly blocked the NGF induction of both HO-1 mRNA (Fig. 6*A*) and protein (Fig. 6*B*) in control EGFP cells. Interestingly, myr-EGFP-Akt1 cells exhibited higher basal levels of HO-1 mRNA (Fig. 6*A*) and protein (Fig. 6*C*) compared with control EGFP cells. Moreover,

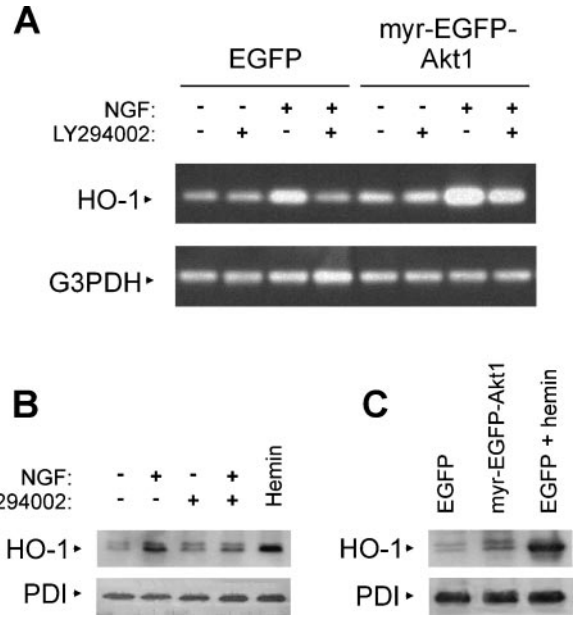

FIG. 6. **NGF induces expression of HO-1 in a PI3K-dependent manner.** *A*, semiquantitative reverse transcriptase-PCR of EGFP and myr-EGFP-Akt1 cells treated with the PI3K inhibitor LY294002 and NGF as indicated. *Upper panel*, HO-1 mRNA; *lower panel*, glyceraldehyde-3-phosphate dehydrogenase (*G3PDH*) mRNA used for normalization. *B*, immunoblots showing a partial block of the NGF-induced increase in HO-1 protein levels in the presence of LY294002. *Upper panel*, immunoblot with anti-HO-1 antibodies; *lower panel*, immunoblot with anti-protein-disulfide isomerase (*PDI*) antibodies showing a similar amount of protein/lane. For *A* and *B*, serum-starved cells were pretreated with 40 μM LY294002 for 15 min and then stimulated with 20 ng/ml NGF for 6 and 12 h, respectively. *C*, immunoblots showing HO-1 protein levels in myr-EGFP-Akt1 cells and in untreated and 50 μM hemin-treated EGFP cells. *Upper panel*, immunoblot with anti-HO-1 antibodies; *lower panel*, immunoblot with anti-protein-disulfide isomerase antibodies showing a similar amount of protein/lane.

the inhibition of PI3K in myr-EGFP-Akt1 cells produced only a small decrease in HO-1 mRNA (Fig. 6*A*), suggesting that myristoylated Akt1 kinase, which does not require 3D′-phosphoinositides for membrane anchorage, is sufficient to activate HO-1 expression. Similar results were obtained when cells were treated with 100 nM wortmannin, another PI3K inhibitor without structural homology to LY294002 (data not shown).

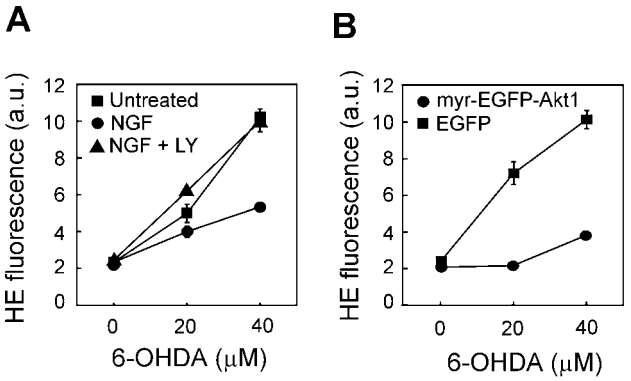

FIG. 7. **The PI3K/Akt pathway mediates attenuation of 6-OHDA-generated ROS.** *A*, the PI3K inhibitor LY294002 prevents attenuation of 6-OHDA-induced ROS by NGF. Serum-starved cells were pretreated with 40 μM LY294002 (*LY*) for 15 min, stimulated with 20 ng/ml NGF for 12 h, and then submitted to a 6-h induction with 6-OHDA and a 1-h incubation with 2 μM HE. HE staining was analyzed by flow cytometry of 10,000 cells/sample. *B*, cells overexpressing active Akt1 exhibit strong attenuation of 6-OHDA-induced production of ROS. Serum-starved EGFP and myr-EGFP-Akt1 cells were treated with 40 μM 6-OHDA for 6 h and with 2 μM HE for 1 h. HE staining was analyzed by flow cytometry of 10,000 cells/sample. *a.u.*, absorbance units.

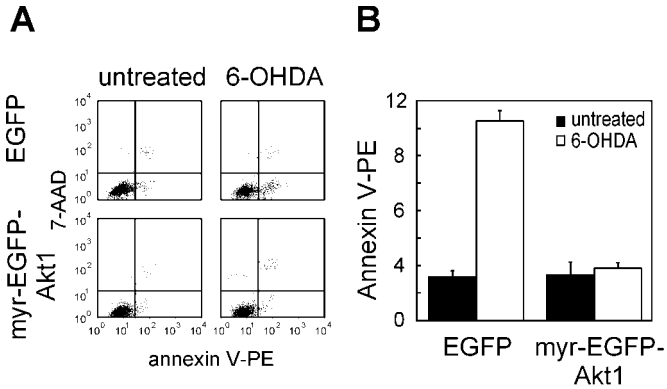

FIG. 8. **Overexpression of membrane-targeted active Akt prevents apoptosis induced by 6-OHDA.** *A*, quantitative determination by flow cytometry of 6-OHDA-induced apoptosis in cells stained with annexin V-PE and 7-AAD. EGFP and myr-EGFP-Akt1 cells were treated with 40 μM 6-OHDA for 6 h and then incubated for 15 min with annexin V-PE (1:20 v/v) and 2 μM 7-AAD. A representative sample of 10,000 cells is shown for each experimental condition. *B*, comparison of the percentage of cells in apoptosis as determined from the *lower right quadrants* in *A*.

Taken together, these results demonstrate that active Akt induces the expression of HO-1 and that NGF regulates the expression of this enzyme, at least in part, through the PI3K/Akt pathway.

The PI3K/Akt Pathway Is Necessary and Sufficient to Attenuate 6-OHDA Generation of ROS—We then analyzed the effect of the PI3K/Akt pathway on the attenuation of 6-OHDA-induced oxidative stress. Serum-starved PC12 cells were pretreated for 15 min with 40 μM LY294002 prior to the addition of NGF. Following a 16-h incubation with NGF, cells were treated with 6-OHDA for 6 h. As shown in Fig. 7*A*, LY294002 reversed the protective effect of NGF against 6-OHDA-induced ROS, further supporting the concept that the PI3K survival pathway controls ROS levels, at least in part, by inducing HO-1 expression. We also analyzed 6-OHDA-induced ROS production in myr-EGFP-Akt1 cells, which harbored higher HO-1 levels compared with control EGFP cells (Fig. 6). As shown in Fig. 7*B*, HE incorporation was fully prevented in myr-EGFP-Akt1 cells at low 6-OHDA concentrations (20 μM) compared with control EGFP cells. At higher concentrations (40 μM), myr-EGFP-Akt1 cells still exhibited a strong attenuation of HE staining. In conclusion, active Akt protects PC12 cells against 6-OHDA-induced oxidative stress, at least in part, by activating the expression of the antioxidant enzyme HO-1.

Active Akt Prevents 6-OHDA-induced Apoptosis—Finally, we investigated whether the deregulated and active form of Akt might attenuate the apoptotic effect of 6-OHDA. We analyzed the loss of plasma membrane asymmetry, which characterizes early apoptosis and results in the exposure of phosphatidylserine to the outer plasma membrane leaflet. This alteration was determined by staining with the phosphatidylserine-binding protein annexin V conjugated to PE. To discriminate early apoptosis from late apoptosis and necrosis, cells were simultaneously stained with 7-AAD, which stains only cells lacking membrane integrity. Serum-starved control EGFP and myr-EGFP-Akt1 cells were submitted to 6 h of incubation with 40 μM 6-OHDA and then stained with annexin V-PE (1:20, v/v) and 2 μM 7-AAD prior to flow cytometric analysis. As shown in Fig. 8*A*, most untreated EGFP and myr-EGFP-Akt1 cells were annexin V-PE- and 7-AAD-negative, indicating that they were viable. However, as shown in Fig. 8*B*, after a 6-h treatment with 40 μM 6-OHDA, ~12% of the EGFP cells were annexin V-PE-positive and 7-AAD-negative, indicating that this population was undergoing early apoptosis. By contrast, the fraction of myr-EGFP-Akt1 cells that were annexin V-PE-positive and 7-AAD-negative after the 6-OHDA insult did not increase significantly. These results indicate that, in addition to attenuation of 6-OHDA-induced oxidative stress, the Akt survival pathway also protects against 6-OHDA-induced apoptosis.

DISCUSSION

This study documents a new physiological role for the PI3K/Akt survival pathway activated by the neurotrophic factor NGF: control of intracellular levels of oxygen free radicals by regulating the expression of HO-1. Previous studies have indicated that NGF elicits a protective effect against oxidative stress both in PC12 cells and in cultured neurons (37, 38). It has also been shown that NGF may modulate the canonical antioxidant machinery of ROS detoxification by increasing the expression of catalase and glutathione peroxidase activities (39, 40). Our experiments further demonstrate that NGF regulates the expression of the novel antioxidant mechanism involving the stress protein HO-1. Moreover, enhanced HO-1 expression is essential for NGF function in ROS detoxification because cells expressing antisense HO-1 retroviral constructs were insensitive to NGF protection against 6-OHDA-induced oxidative stress. Although PI3K/Akt is a well documented pathway involved in protecting against apoptosis insults, including oxidative stress, this is the first report linking this survival pathway with a specific enzyme involved in ROS detoxification of mammalian cells. We show that the PI3K/Akt pathway is both necessary and sufficient for NGF-dependent abrogation of ROS levels in PC12 cells exposed to 6-OHDA.

The protective role of the stress protein HO-1 in the brain has not been accepted until recently. Initially, post-mortem examination of human brain specimens revealed that expression of HO-1 immunoreactivity decorates Lewy bodies in the substantia nigra of Parkinson's patients (23). This led to the assumption that HO-1 overactivity might not protect, but rather contribute to the development of parkinsonism because iron accumulation in dopaminergic neurons may contribute to chronic oxidative damage, leading to neurodegeneration in Parkinson's patients. A protective role for HO catabolism in the nervous system has been also challenged by the fact that hyperbilirubinemia is commonly associated with nerve cell injury and brain damage during severe neonatal jaundice and Crigler-Najjar type II syndrome (41, 42). Consistent with these obser-

vations, we could not obtain high constitutive levels of HO-1 expression either in HO-1-overexpressing cells (2.3-fold) or in myr-EGFP-Akt1 cells (2.5-fold). It is interesting, however, that short-term stimulation with NGF or other inducers of HO-1 such as hemin and $CoCl_2$ may yield much higher transient levels of HO-1 expression. These observations are in agreement with the notion that HO-1 is a stress response protein (HSP32).

Therefore, a key point toward establishing the protective or noxious effect on the HO system under conditions of oxidative injury may be related to the relative abundance of HO enzymes and their products. Low concentrations of bilirubin derived from HO-2 overexpression protect against neuronal oxidant injury (43), and moderated levels of bilirubin exert antioxidant actions in the neonate and protect against retinopathy in premature newborns (44). Likewise, recent reports have shown that transgenic mice overexpressing moderate levels of HO-1 display augmented resistance to neural damage in animal models of cerebral ischemia (45) or after H_2O_2- and glutamate-induced oxidant stress *in vitro* (24). Accordingly, we have shown that constitutive but moderate overexpression of HO-1 attenuated 6-OHDA-induced ROS generation.

The HO-1 gene contains a complex promoter with a large variety of regulatory elements (46). Some of these sequences might be putative candidates for regulation by PI3K and Akt. As a heat shock protein, the promoter of HO-1 contains several heat shock elements that may be negatively regulated by glycogen synthase kinase-3-mediated phosphorylation of heat shock factor-1. Because Akt phosphorylates and inhibits glycogen synthase kinase-3 (47), these might be sites of indirect regulation by this pathway. Another putative site involves the antioxidant-responsive element. During oxidative stress, the basic leucine zipper transcription factor Nrf2 heterodimerizes with small Maf to bind and activate antioxidant-responsive element sequences (48). Although the putative regulation of Nrf2 by PI3K is poorly defined, recent reports suggest that PI3K regulates nuclear translocation of Nrf2 through actin rearrangement in response to oxidative stress (49). We are currently analyzing these and other promoter regions that might ultimately respond to PI3K/Akt regulation.

Given the variety of enzymes involved in oxidative detoxification, a striking finding of this study is the strong dependence on HO-1 to protect against 6-OHDA-induced oxidative stress. This may be explained by considering the mechanism involved in 6-OHDA toxicity. Probably, H_2O_2 is the most abundant form of ROS generated by 6-OHDA (25), and bilirubin is particularly well suited to deal with this compound because nanomolar amounts of bilirubin reduce micromolar amounts of H_2O_2 (43). Moreover, other antioxidant enzymes may be regulated by byproducts of HO-1 activity, thus contributing to ROS detoxification. For example, HO-1 activates the expression of mitochondrial superoxide dismutase in neonatal rat astroglia challenged with dopamine (50).

Finally, we discovered that membrane-targeted active Akt prevented the effects of 6-OHDA not only on ROS production, but also on apoptosis, further suggesting that moderate overexpression of HO-1 through the PI3K/Akt survival pathway may be an important element for prevention of both phenomena. Considering the importance of apoptosis and ROS in neurodegeneration, this study suggests that activation of the PI3K/Akt pathway might have a therapeutic use in the treatment of oxidative stress-related neurodegenerative disorders such as Parkinson's disease.

REFERENCES

1. Pettmann, B., and Henderson, C. E. (1998) *Neuron* **20,** 633–647
2. Wiesmann, C., Ultsch, M. H., Bass, S. H., and de Vos, A. M. (1999) *Nature* **401,** 184–188
3. Kaplan, D. R., and Miller, F. D. (2000) *Curr. Opin. Neurobiol.* **10,** 381–391
4. Brazil, D. P., and Hemmings, B. A. (2001) *Trends Biochem. Sci.* **26,** 657–664
5. Burgering, B. M., and Kops, G. J. (2002) *Trends Biochem. Sci.* **27,** 352–360
6. Brunet, A., Datta, S. R., and Greenberg, M. E. (2001) *Curr. Opin. Neurobiol.* **11,** 297–305
7. Goldshmit, Y., Erlich, S., and Pinkas-Kramarski, R. (2001) *J. Biol. Chem.* **276,** 46379–46385
8. Ikeyama, S., Kokkonen, G., Shack, S., Wang, X. T., and Holbrook, N. J. (2002) *FASEB J.* **16,** 114–116
9. Martín, D., Salinas, M., Lopez-Valdaliso, R., Serrano, E., Recuero, M., and Cuadrado, A. (2001) *J. Neurochem.* **78,** 1000–1008
10. Salinas, M., Martín, D., Alvarez, A., and Cuadrado, A. (2001) *Mol. Cell. Neurosci.* **17,** 67–77
11. Martín, D., Salinas, M., Fujita, N., Tsuruo, T., and Cuadrado, A. (2002) *J. Biol. Chem.* **277,** 42943–42952
12. Honda, Y., and Honda, S. (1999) *FASEB J.* **13,** 1385–1393
13. Kops, G. J., Dansen, T. B., Polderman, P. E., Saarloos, I., Wirtz, K. W. A., Coffer, P. J., Huang, T. T., Bos, J. L., Medena, R. H., and Burgering, B. M. T. (2002) *Nature* **419,** 316–321
14. Tabú, J., Lau, J. F., Ma, C., Hahn, J. H., Hoque, R., Rothblatt, J., and Chalfie, M. (1999) *Nature* **399,** 162–166
15. Clancy, D. J., Gems, D., Harshman, L. G., Oldham, S., Stocker, H., Hafen, E., Leevers, S. J., and Partridge, L. (2001) *Science* **292,** 104–106
16. Morse, D., and Choi, A. M. (2002) *Am. J. Respir. Cell Mol. Biol.* **27,** 8–16
17. Otterbein, L. E., and Choi, A. M. (2000) *Am. J. Physiol.* **279,** L1029–L1037
18. Baranano, D. E., and Snyder, S. H. (2001) *Proc. Natl. Acad. Sci. U. S. A.* **98,** 10996–11002
19. Dennery, P. A. (2000) *Curr. Top. Cell. Regul.* **36,** 181–199
20. Ewing, J. F., Haber, S. N., and Maines, M. D. (1992) *J. Neurochem.* **58,** 1140–1149
21. Takeda, A., Onodera, H., Sugimoto, A., Itoyama, Y., Kogure, K., and Shibahara, S. (1994) *Brain Res.* **666,** 120–124
22. Takeda, A., Perry, G., Abraham, N. G., Dwyer, B. E., Kutty, R. K., Laitinen, J. T., Petersen, R. B., and Smith, M. A. (2000) *J. Biol. Chem.* **275,** 5395–5399
23. Schipper, H. M., Liberman, A., and Stopa, E. G. (1998) *Exp. Neurol.* **150,** 60–68
24. Chen, K., Gunter, K., and Maines, M. D. (2000) *J. Neurochem.* **75,** 304–313
25. Blum, D., Torch, S., Lambeng, N., Nissou, M., Benabid, A. L., Sadoul, R., and Verna, J. M. (2001) *Prog. Neurobiol.* **65,** 135–172
26. Lotharius, J., Dugan, L. L., and O'Malley, K. L. (1999) *J. Neurosci.* **19,** 1284–1293
27. Quan, S., Yang, L., Abraham, N. G., and Kappas, A. (2001) *Proc. Natl. Acad. Sci. U. S. A.* **98,** 12203–12208
28. Ryter, S. W., Kvam, E., and Tyrrell, R. M. (2000) *Methods Mol. Biol.* **99,** 369–391
29. Chomczynski, P., and Sacchi, N. (1987) *Anal. Biochem.* **162,** 156–159
30. Bindokas, V. P., Jordan, J., Lee, C. C., and Miller, R. J. (1996) *J. Neurosci.* **16,** 1324–1336
31. Bindokas, V. P., Kuznetsov, A., Sreenan, S., Polonsky, K. S., Roe, M. W., and Philipson, L. H. (2003) *J. Biol. Chem.* **278,** 9796–9801
32. Ohashi, T., Mizutani, A., Murakami, A., Kojo, S., Ishii, T., and Taketani, S. (2002) *FEBS Lett.* **511,** 21–27
33. Chen, K., and Maines, M. D. (2000) *Cell. Mol. Biol.* **46,** 609–617
34. Hill-Kapturczak, N., Truong, L., Thamilselvan, V., Visner, G. A, Nick, H. S., and Agarwal, A. (2000) *J. Biol. Chem.* **275,** 40904–40909
35. Llesuy, S. F., and Tomaro, M. L. (1994) *Biochim. Biophys. Acta* **1223,** 9–14
36. Li Volti, G., Wang, J., Traganos, F., Kappas, A., and Abraham, N. G. (2002) *Biochem. Biophys. Res. Commun.* **296,** 1077–1082
37. Wang, W., Post, J. I., Dow, K. E., Shin, S. H., Riopelle, R. J., and Ross, G. M. (1999) *Neurosci. Lett.* **259,** 115–118
38. Kirschner, P. B., Jenkins, B. G., Schulz, J. B., Finkelstein, S. P., Matthews, R. T., Rosen, B. R., and Beal, M. F. (1996) *Brain Res.* **713,** 178–185
39. Satoh, T., Yamagata, T., Ishikawa, Y., Yamada, M., Uchiyama, Y., and Hatanaka, H. (1999) *J. Biochem.* (*Tokyo*) **125,** 952–959
40. Sampath, D., and Perez-Polo, R. (1997) *Neurochem. Res.* **22,** 351–362
41. Gourley, G. R. (1997) *Adv. Pediatr.* **44,** 173–229
42. Rubboli, G., Ronchi, F., Cecchi, P., Rizzi, R., Gardella, E., Meletti, S., Zaniboni, A., Volpi, L., and Tassinari, C. A. (1997) *Neuropediatrics* **28,** 281–286
43. Dore, S., Takahashi, M., Ferris, C. D., Zakhary, R., Hester, L. D., Guastella, D., and Snyder, S. H. (1999) *Proc. Natl. Acad. Sci. U. S. A.* **96,** 2445–2450
44. Hegyi, T., Goldie, E., and Hiatt, M. (1994) *J. Perinatol.* **14,** 296–300
45. Panahian, N., Yoshiura, M., and Maines, M. D. (1999) *J. Neurochem.* **72,** 1187–1203
46. Elbirt, K. K., and Bonkovsky, H. L. (1999) *Proc. Assoc. Am. Physicians* **111,** 438–447
47. Xavier, I. J., Mercier, P. A., McLoughlin, C. M., Ali, A., Woodgett, J. R., and Ovsenek, N. (2000) *J. Biol. Chem.* **275,** 29147–29152
48. Kataoka, K., Handa, H., and Nishizawa, M. (2001) *J. Biol. Chem.* **276,** 34074–34081
49. Kang, K. W., Lee, S. J., Park, J. W., and Kim, S. G. (2002) *Mol. Pharmacol.* **62,** 1001–1010
50. Frankel, D., Mehindate, K., and Schipper, H. M. (2000) *J. Cell. Physiol.* **185,** 80–86

Nerve Growth Factor Protects against 6-Hydroxydopamine-induced Oxidative Stress by Increasing Expression of Heme Oxygenase-1 in a Phosphatidylinositol 3-Kinase-dependent Manner

Marta Salinas, Raquel Diaz, Nader G. Abraham, Carlos M. Ruiz de Galarreta and Antonio Cuadrado

J. Biol. Chem. 2003, 278:13898-13904.
doi: 10.1074/jbc.M209164200 originally published online February 10, 2003
